The Cryosphere Discuss., 8, 1257–1278, 2014
www.the-cryosphere-discuss.net/8/1257/2014/
doi:10.5194/tcd-8-1257-2014

The Cryosphere
Discussions
Open Access

Glacier dynamics at Helheim and Kangerdlugssuaq glaciers, southeast Greenland, since the Little Ice Age

S. A. Khan[1], **K. K. Kjeldsen**[2], **K. H. Kjær**[2], **S. Bevan**[3], **A. Luckman**[3], **A. Aschwanden**[4], **N. J. Korsgaard**[2], **A. A. Bjørk**[2], **J. Box**[5], **M. van den Broeke**[6], **T. M. van Dam**[7], **and A. Fitzner**[8]

[1]DTU Space – National Space Institute, Technical University of Denmark, Department of Geodesy, Kgs. Lyngby, Denmark
[2]Centre for GeoGenetics, Natural History Museum, University of Copenhagen, Copenhagen, Denmark
[3]Geography Department, College of Science, Swansea University, Swansea, UK
[4]Geophysical Institute, University of Alaska Fairbanks, USA
[5]Geological Survey of Denmark and Greenland, Copenhagen, Denmark
[6]Institute for Marine and Atmospheric Research, Utrecht University, Utrecht, the Netherlands
[7]Faculté des Sciences, de la Technologie et de la Communication, University of Luxembourg, Luxembourg
[8]Centre for Ice and Climate, University of Copenhagen, Copenhagen, Denmark

Received: 23 January 2014 – Accepted: 4 February 2014 – Published: 21 February 2014

Correspondence to: S. A. Khan (abbas@space.dtu.dk)

Published by Copernicus Publications on behalf of the European Geosciences Union.

Abstract

Observations over the past decade show significant ice loss associated with the speed-up of glaciers in southeast Greenland from 2003, followed by a deceleration from 2006. These short-term, episodic, dynamic perturbations have a major impact on the mass balance at the decadal scale. To improve the projection of future sea level rise, a long-term data record that reveals the mass balance beyond such episodic events is required. Here, we extend the observational record of marginal thinning of Helheim glacier (HG) and Kangerdlugssuaq glacier (KG) from 10 to more than 150 yr. We show that although the frontal portion of HG thinned by more than 100 m between 2003 and 2006, it thickened by more than 50 m during the previous two decades. In contrast, KG was stable from 1981 to 1998 and experienced major thinning only after 2003. Extending the record back to the end of the Little Ice Age (ca. 1850) shows no significant thinning of HG from 1850 to 1981, while KG underwent substantial thinning of ~265 m. Analyses of their sensitivity to sub-surface water temperature anomalies and variations in air temperature suggest that both HG and KG are highly sensitive to short-term atmospheric and ocean forcing, and respond very quickly to small fluctuations. At century time-scales, however, multiple external parameters (e.g. outlet shape) dominate the mass change. These findings undermine attempts to use measurements over the last decade as initial conditions to project future dynamic ice loss.

1 Introduction

Since 2003, more than 50 % of the total ice loss of the Greenland Ice Sheet (GrIS) occurred in southeast Greenland (Chen et al., 2011; Khan et al., 2010; Luthcke et al., 2006; Rignot et al., 2008; Stearns and Hamilton, 2007; Velicogna and Wahr, 2006; van den Broeke et al., 2009). Two of the largest outlet glaciers in this region, HG and KG, with a total catchment-wide drainage area of about 250×10^3 km^2 (Fig. 1), contributed up to 122 km^3 yr^{-1} of ice loss (Luckman et al., 2006; Stearns and Hamilton, 2007; Khan et al., 2007), which is itself more than half of the southeast Greenland total (Joughin et al., 2010; Luthcke et al., 2006; Velicogna and Wahr, 2006), indicating the particular importance of these two major outlet glaciers.

The mass loss of the GrIS has accelerated due to a combination of increased ice velocity (Howat et al., 2007; Joughin et al., 2010; Luckman et al., 2006; Pritchard et al., 2009; Rignot et al., 2008) causing dynamic ice loss, and a warmer atmosphere (van den Broeke et al., 2009) leading to enhanced surface meltwater runoff. Recent model results use data from the last decade as initial conditions to model GrIS's contribution to sea level rise by 2100 (Enderlin et al., 2013; Nick et al., 2013; Price et al., 2011). The last decade, however, is not necessarily typical of conditions at these glaciers and appears to have been dominated by anomalous dynamic behaviour (Bevan et al., 2012). Improved projections of ice sheets future contributions to global sea level change require longer-term data records that reveal the mass balance beyond the last decade, and a better understanding of the sensitivity of dynamic thinning to climate forcing on decadal time scales. Here we extend the observational record of marginal thinning to more than a century for the two most prominent outlet glaciers in southeast Greenland, HG and KG. We analyse marginal changes between the LIA maximum (Lowell, 2000) and 2012, and test their sensitivity to Sub-surface water temperature (SSWT) anomalies and variations in air temperature.

2 Data

2.1 Surface elevation

To map changes in HG and KG we use altimeter surveys from NASA's Airborne Topographic Mapper (ATM) flights during 1993–2011 (Krabill, 2012), supplemented with high resolution Ice, Cloud and land Elevation Satellite (ICESat) laser altimeter data (Zwally et al., 2012) from 2003 to 2009. To assess thinning prior to 1993, we analyse 1981 aerial photos covering the frontal portion of HG and KG (Fig. 2). The Aerial pho-

TCD
8, 1257–1278, 2014

tographs of HG and KG were recorded between 30 July and 14 August 1981 by the Danish Geodata Agency in order to provide stereoscopic coverage of ice-free terrain including nunataks. The scale is 1 : 150 000. Ground control points (list of coordinates) and image observations were provided by the Danish Geodata Agency. The coordinate list is in the Greenland 1996 reference system (GR96). Heights are mean sea level heights, and these were transformed to ellipsoid heights for our purposes. SOCET SET 5.5 (BAE Systems) and ArcGIS 10 (Esri) were used to process the data. We use these data to derive a 25×25 m gridded DEM for 1981 in a Universal Transverse Mercator (UTM) coordinate system (zone 24) with elevations referenced to the height above the ellipsoid (World Geodetic System 1984). We generated the DEMs for the two regions from 27 photos (see Fig. 2). The coordinate list contains 233 ground control points with coordinates derived from the GR96 aero-analytical triangulation using geodetically surveyed stations for geo-location.

2.2 Ice flow speeds

Surface flow speeds were measured by applying feature tracking to repeat-pass satellite images including Landsat-5 (Band 4), Landsat-7 (Band 8), ERS-1 SAR, ERS-2 SAR and Envisat ASAR (Bevan et al., 2012). Optical pairs were separated by 16 or 32 days, SAR pairs by 35 days, and errors are estimated to be less than 0.2 m/day.

2.3 Ocean and air temperature

Figure 3 shows annual mean sub-surface water temperature (SSWT) anomalies obtained from the Hadley Centre EN3 model output (http://www.metoffice.gov.uk/hadobs/en3/). We use objective analyses based on optimal interpolation of the in situ data profiles combined with a quality control system (Ingleby and Huddleston, 2007). We remove the 1981–2012 mean temperature to obtain the anomalies. HG and KG is situated on a broad continental shelf (Bamber et al., 2013), therefore, water depth is limited to few hundred meters. Consequently, we use data in the EN3 model at 315 m depth.

Air temperature records for the two stations used in this study are obtained from The Danish Meteorological Institute (DMI) (Boas and Wang, 2011). The northern record close to KG (∼ 80 km) is comprised of data from two coastal stations at Apuiteeq (13 m above sea-level), station 04350 which operated until 1987 and station 04351 which replaced it at the same location. The meteorological station is very remote, hence, a long time can pass when instruments fail before they can be replaced. This has led to the blanks in the temperature record (1986, 2003, 2004, 2006, and 2007). The temperature record close to HG is the station 04360 located in the town of Tasiilaq (∼ 50 m above sea-level) ∼ 85 km from HG. Data is available from DMI (Boas and Wang, 2011). We use the mean temperature during 1981–2012 to produce temperature anomalies.

3 Method

To estimate elevation change, we use ICESat and ATM track points that are less than 17 m from the nearest measured 1981 DEM point (i.e. within one DEM pixel) so that surface slope can be ignored. Combining our error estimates (RMS), the thinning values for HG and KG (shown in Figs. 4 and 5) have uncertainties of 5.1 m and 9.4 m, respectively (the uncertainties are derived using the same method as Khan et al., 2013; Kjær et al., 2012; Motyka et al., 2010).

To extend the observational record to the century timescale we use the so-called "historical moraines", i.e. fresh non-vegetated moraines close to the present glacier fronts seen in many parts of Greenland, and fresh trimlines, i.e. pronounced boundaries between abraded and less abraded bedrock on valley sides (Csatho et al., 2008). These mark the culmination of LIA glacier advances and formed during the end of the LIA c. 1850 (Lowell, 2000). The vertical aerial stereo photographs from 1981 were processed using the SOCETset software package. This allows a 3-D-mapping of features outlining the Little Ice Age maximum (LIA_{max}) extent. Each sample location contains two data points placed perpendicular to the flow direction; one being the elevation of the LIA_{max} extent and the other being the elevation of the 1981 ice surface (see Fig. 6).

TCD
8, 1257–1278, 2014

The vertical difference (dh_{LIA}) is determined from these two data points; hence, we assume that the cross-section profile of the glacier is the same during the LIA_{max} and 1981. The uncertainty of thinning between 1850 and 1981 can be expressed as the uncertainty between two points on the 1981 DEM, $\sigma_{LIA} = \sqrt{\sigma^2_{DEM1981} + \sigma^2_{DEM1981}} = 7.2\,m$ (for HG) and 13.3 m (for KG)

4 Results and discussion

4.1 Thinning during 1981–2012

On HG we measure a thickening of 50–60 m along the satellite track line between 1981 and 1997 (Fig. 4a and 7a). Thickening of the glacier front continued until 1998, followed by a moderate thinning from 1998 to 2003, by which time the frontal portion had returned to the 1981 elevation. Rapid thinning continued until 2006, when the frontal portion was > 70 m lower than the 1981 elevation or > 130 m lower than in 1998. From 2006 to 2012 HG experienced modest thickening because the ice front had retreated beyond an overdeepening at the glacier bed (Nick et al., 2013; Price et al., 2011).

In contrast to HG, KG shows no significant elevation changes, driven dynamically or by melt, from 1981 to 1993 (Figs. 5a and 7b). Thinning commenced between 1993 and 1998 by which time the glacier had thinned by 20–25 m, and continued by an additional 15–20 m until 2001 (Fig. 5a–c). Only small changes of 5–10 m were observed between 2001 and 2003. Major thinning of more than 100 m occurred from 2003 to 2007, followed by more moderate fluctuations (Fig. 7b and d). The timing of dynamic thinning is consistent with changes in observed surface flow speed (Fig. 7c and d).

To isolate dynamically induced elevation changes, we use the BOX model (Box, 2013) to predict elevation changes due to Surface Mass Balance (SMB) fluctuations. SMB, equal to net snow accumulation minus snow and ice meltwater runoff was reconstructed on a 5 km grid for Greenland ice spanning 1840–2010 (Box, 2013). Reconstructed SMB is validated using data from the K-transect (van de Wal et al., 2012)

TCD
8, 1257–1278, 2014

along the western ice sheet and has an RMSE of roughly 0.45 m water equivalence. Periods of slow down and speed up (Fig. 7c and d) agree very well with the estimates of dynamic thickening/thinning on both glaciers (Fig. 7a, b).

4.2 Ocean and air temperature

Figure 7e and f shows annual mean SSWT anomalies at point 1 (lat = 65.5° N, lon = 36.5° W) and 2 (lat = 67.5° N, lon = 31.5° W) (see Fig. 1). Ocean and atmospheric temperatures are relatively low until the late 1990's after which they are consistently higher. The relatively colder water and air during 1981–1998 occurred when the frontal portion of HG thickened by ~ 60 m. The start of the somewhat warmer climate in 1998 seems to have halted the thickening of the glacier and instead started a rapid reversal of the process. Our results suggest that HG is very sensitive to even small fluctuations in the SSWT and air temperature. The simultaneous increase of SSWT and air temperature likely enhanced thinning of HG. Rates of submarine melting increase significantly in the presence of subglacial meltwater plumes in front of calving termini (Motyka et al., 2003; Rignot et al., 2010). The plumes promote melt because they introduce turbulent transfers at the ice/ocean boundary (Jenkins et al., 2010; Seale et al., 2011). Even though KG experienced roughly the same climate forcing as HG (see Fig. 7e–h), no thickening occurred during the relative cold period from 1981 to 1998. However, higher ocean and air temperatures from 1998 onward caused enhanced and rapid dynamic thinning.

4.3 Thinning since the Little Ice Age

At both HG and KG surface elevation and surface flow speed appear to be forced by atmospheric and oceanic changes. On short timescales both glaciers respond very quickly to atmospheric and oceanic fluctuations. To extend the observational record to the century timescale we use the historical moraines and fresh trimlines. Our results suggest HG experienced no significant elevation change between 1850 and 1981

TCD
8, 1257–1278, 2014

(Fig. 1c), while KG thinned by ∼ 265 m during the same period (Fig. 1b). The frontal position of HG retreated from 1850 to the late 1930s, and has since advanced/retreated several times until 1981 (Bjørk et al., 2012) (see Fig. 8). Hence, HG likely experienced several periods of dynamic thinning and thickening; however, the overall elevation change during 1850–1981 is close to zero. In contrast, KG experienced major thinning and retreat (Figs. 1b and 9). Though HG and KG appear to respond similarly to short-term oceanic and atmospheric forcing, they exhibit quite different long-term behavior suggesting other forcing parameters may dominate the mass budget at century timescales. Sensitivity tests to outlet shape suggest small variations in bed topography can result in either stable or unstable retreat/advance due to the same perturbation (Enderlin et al., 2013).

5 Conclusions

Our results suggest HG experienced no significant net elevation change during 1850–1981, while KG underwent substantial thinning of ∼ 265 m. In the early 1930s the marginal position of KG was very close to the LIA maximum position, and during the course of a single year from 1932–1933 the advanced floating tongue collapsed and the front retreated more than 7 kilometers (Wager et al., 1937; Spender, 1933), marking the onset of the KG's 20th Century thinning. From the LIA maximum to 2012 the frontal portion of KG thinned by more than 500 m.

KG has a bed which deepens inland and the glacier front has retreated throughout the last century (see Fig. 9). HG has retreated several times throughout the last century, however, likely due to an overdeepening, the retreats have been followed by advances (e.g. during 2005–2006).

Although atmospheric and oceanic forcing is able to capture changes at multi-year time-scales very well (Nick et al., 2013; Price et al., 2011), our measurements show that dynamic ice loss is more complex than hypothesized. At century time-scales, multiple external parameters (e.g. bed elevation, width and/or grounding line migration, Jamieson et al., 2012) dominate the mass change. These findings suggest that long-term data record as initial conditions that capture the mass balance between episodic events is required to extrapolate mass-balance estimates into the future.

Acknowledgements. Shfaqat Abbas Khan was supported by the Danish Council for Independent Research – Nature and Universe.

References

Bamber, J. L., Griggs, J. A., Hurkmans, R. T. W. L., Dowdeswell, J. A., Gogineni, S. P., Howat, I., Mouginot, J., Paden, J., Palmer, S., Rignot, E., and Steinhage, D.: A new bed elevation dataset for Greenland, The Cryosphere, 7, 499–510, doi:10.5194/tc-7-499-2013, 2013.

Bevan, S. L., Luckman, A. J., and Murray, T.: Glacier dynamics over the last quarter of a century at Helheim, Kangerdlugssuaq and 14 other major Greenland outlet glaciers, The Cryosphere, 6, 923–937, doi:10.5194/tc-6-923-2012, 2012.

Bjørk, A. A., Kjær, K. H., Korsgaard, N. J., Khan, S. A., Kjeldsen, K. K., Andresen, C. S., Box, J. E., Larsen, N. K., and Funder, S.: An aerial view of 80 years of climate-related glacier fluctuations in southeast Greenland, Nat. Geosci., 5, 427–432, doi:10.1038/ngeo1481, 2012.

Boas, L. and Wang, P. R.: Weather and climate data from Greenland 1958–2010, Danish Meteorological Institute, Copenhagen, DMI Technical Report 11–15, 2011.

Box, J. E.: Greenland ice sheet mass balance reconstruction, Part II: Surface mass balance (1840–2010), J. Climate, 26, 6974–6989, 2013.

Csatho, B., Schenk, T., Van Der Veen, C. J., and Krabill, W. B.: Intermittent thinning of Jakobshavn Isbræ, West Greenland, since the Little Ice Age, J. Glaciol., 54, 131–144, 2008.

Chen, J. L., Wilson, C. R., and Tapley, B. D.: Interannual variability of Greenland ice losses from satellite gravimetry, J. Geophys. Res., 116, B07406, doi:10.1029/2010JB007789, 2011.

Enderlin, E. M., Howat, I. M., and Vieli, A.: High sensitivity of tidewater outlet glacier dynamics to shape, The Cryosphere, 7, 1007–1015, doi:10.5194/tc-7-1007-2013, 2013.

Howat, I. M., Joughin, I., and Scambos, T. A.: Rapid changes in ice discharge from Greenland outlet glaciers, Science, 315, 1559–1561, 2007.

Ingleby, B. and Huddleston, M.: Quality control of ocean temperature and salinity profiles – historical and real-time data, J. Marine Syst., 65, 158–175, doi:10.1016/j.jmarsys.2005.11.019, 2007.
Jamieson, S. S. R., Vieli, A., Livingstone, S. J., Cofaigh, C., Stokes, C., Hillenbrand, C.-D., and Dowdeswell, J. A.: Ice-stream stability on a reverse bed slope, Nat. Geosci., 5, 799–802, 2012.
Jenkins, A., Nicholls, K. W., and Corr, H. F. J.: Observation and parameterization of ablation at the base of Ronne Ice Shelf, Antarctica, J. Phys. Oceanogr., 40, 2298–2311, 2010.
Joughin, I., Smith, B. E., Howat, I. M., Scambos, T., and Moon, T.: Greenland flow variability from ice-sheet-wide velocity mapping, J. Glaciol., 56, 415–430, 2010.
Khan, S. A., Wahr, J., Stearns, L. A., Hamilton, G. S., van Dam, T., Larson, K. M., and Francis, O.: Elastic uplift in southeast Greenland due to rapid ice mass loss, Geophys. Res. Lett., 34, L21701, doi:10.1029/2007GL031468, 2007.
Khan, S. A., Wahr, J., Bevis, M., Velicogna, I., and Kendrick, E.: Spread of ice mass loss into northwest Greenland observed by GRACE and GPS, Geophys. Res. Lett., 37, L06501, doi:10.1029/2010GL042460, 2010.
Khan, S. A., Kjær, K. H., Korsgaard, N. J., Wahr, J., Joughin, I. R., Timm, L. H., Bamber, J. L., van den Broeke, M. R., Stearns, L. A., Hamilton, G. S., Csatho, B. M., Nielsen, K., Hurkmans, R., and Babonis, G.: Recurring dynamically induced thinning during 1985 to 2010 on Upernavik Isstrøm, West Greenland, J. Geophys. Res.-Earth, 118, 111–121, doi:10.1029/2012JF002481, 2013.
Kjær, K. H., Khan, S. A., Korsgaard, N. J., Wahr, J., Bamber, J. L., Hurkmans, R., van den Broeke, M., Timm, L. H., Kjeldsen, K. K., Bjork, A. A., Larsen, N. K., Jørgensen, L. T., Færch-Jensen, A., and Willerslev, E.: Aerial photographs reveal late-20th-century dynamic ice loss in Northwestern Greenland, Science, 337, 569–573, doi:10.1126/science.1220614, 2012.
Krabill, W. B.: IceBridge ATM L2 Icessn Elevation, Slope, and Roughness, [1993–2012], Boulder, Colorado USA: NASA Distributed Active Archive Center at the National Snow and Ice Data Center. Digital media. http://nsidc.org/data/ilatm2.html (last access: 13 February 2014), 2012.
Lowell, T. V.: As climate changes, so do glaciers, P. Natl. Acad. Sci. USA, 97, 1351–1354, 2000.
Luthcke, S. B., Zwally, H. J., Abdalati, W., Rowlands, D. D., Ray, R. D., Nerem, R. S., Lemoine, F. G., McCarthy, J. J., and Chinn, D. S.: Recent Greenland ice mass loss by drainage system from satellite gravity observations, Science, 314, 1286–1289, 2006.

TCD
8, 1257–1278, 2014

Luckman, A., Murray, T., de Lange, R., and Hanna, E.: Rapid and synchronous ice-dynamic changes in east Greenland, Geophys. Res. Lett., 33, L03503, doi:10.1029/2005GL025428, 2006.
Motyka, R. J., Hunter, L., Echelmeyer, K. A., and Connor, C.: Submarine melting at the terminus of a temperate tidewater glacier, LeConte Glacier, Alaska, USA, Ann. Glaciol., 36, 57–65, doi:10.3189/172756403781816374, 2003.
Motyka, R. J., Fahnestock, M., and Truffer, M.: Volume change of Jakobshavn Isbræ, West Greenland: 1985–1997–2007, J. Glaciol., 56, 635–646, doi:10.3189/002214310793146304, 2010.
Nick, F., Vieli, A., Andersen, M. L., Joughin, I., Payne, A., Edwards, T. L., Pattyn, F., and van deWal, R. S. W.: Future sea-level rise from Greenland's main outlet glaciers in a warming climate, Nature, 497, 235–238, doi:10.1038/nature12068, 2013.
Price, S. F., Payne, A. J., Howat, I. M., and Smith, B. E.: Committed sea-level rise for the next century from Greenland ice sheet dynamics during the past decade, P. Natl. Acad. Sci. USA, 108, 8978–8983, doi:10.1073/pnas.1017313108, 2011.
Pritchard, H. D., Arthern, R. J. Vaughan, D. G., and Edwards, L. A.: Extensive dynamic thinning on the margins of the Greenland and Antarctic ice sheets, Nature, 461, 971–975, 2009.
Rignot, E., Box, J. E., Burgess, E., and Hanna, E.: Mass balance of the Greenland ice sheet from 1958 to 2007, Geophys. Res. Lett., 35, L20502, doi:10.1029/2008GL035417, 2008.
Rignot, E., Koppes, M., and Velicogna, I.: Rapid submarine melting of the calving faces of West Greenland glaciers, Nat. Geosci., 3, 187–191, doi:10.1038/ngeo765, 2010.
Seale, A., Christoffersen, P., Mugford, R. I., and O'Leary, M.: Ocean forcing of the Greenland Ice Sheet: Calving fronts and patterns of retreat identified by automatic satellite monitoring of eastern outlet glaciers, J. Geophys. Res., 116, F03013, doi:10.1029/2010JF001847, 2011.
Spender, M.: Mapmaking during the Expedition, Meddelelser om Grønland, 104, 1–21, 1933.
Stearns, L. A. and Hamilton, G. S.: Rapid volume loss from two East Greenland outlet glaciers quantified using repeat stereo satellite imagery, Geophys. Res. Lett., 34, L05503, doi:10.1029/2006GL028982, 2007.
Van den Broeke, M. R., Bamber, J., Ettema, J., Rignot, E., Schrama, E., van de Berg, W. J., van Meijgaard, E., Velicogna, I., and Wouters, B.: Partitioning recent Greenland mass loss, Science, 326, 984–986, 2009.

TCD
8, 1257–1278, 2014

van de Wal, R. S. W., Boot, W., Smeets, C. J. P. P., Snellen, H., van den Broeke, M. R., and Oerlemans, J.: Twenty-one years of mass balance observations along the K-transect, West Greenland, Earth Syst. Sci. Data, 5, 351–363, doi:10.5194/essdd-5-351-2012, 2012.
Velicogna, I. and Wahr, J.: Acceleration of Greenland ice mass loss in spring 2004, Nature, 443, 7109, 329–331, 2006.
Wager, L., Deer, W., Wager, H., and Manley, G.: The Kangerdlugssuak Region of East Greenland, Geogr. J., 90, 393–421, 1937.
Zwally, H. J., Schutz, R., Bentley, C., Bufton, J., Herring, T., Minster, J., Spinhirne, J., and Thomas, R., GLAS/ICESat L2 Antarctic and Greenland Ice Sheet Altimetry Data V031, NASA Distributed Active Archive Center at the National Snow and Ice Data Center, Digital media, Boulder, Colorado, 2012.

TCD
8, 1257–1278, 2014

Glacier dynamics at Helheim and Kangerdlugssuaq glaciers

S. A. Khan et al.

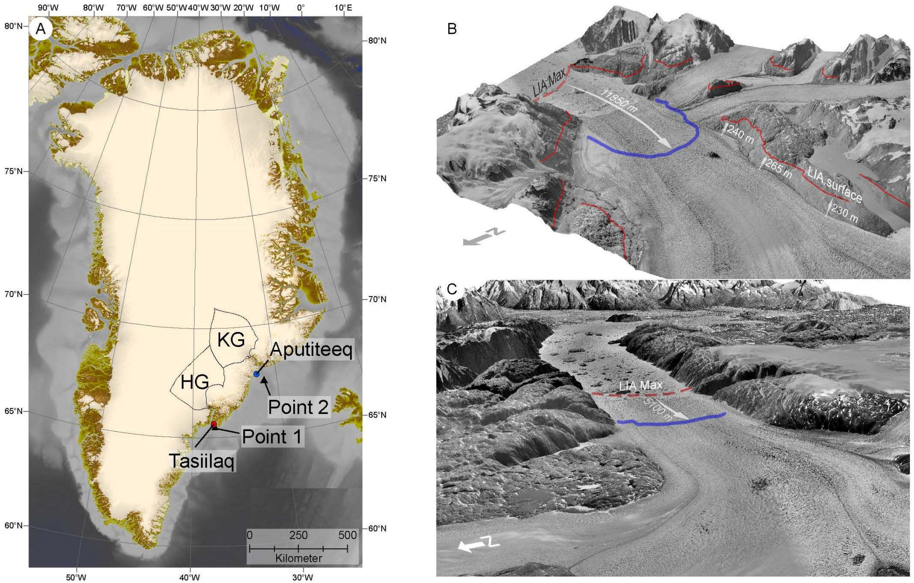

Fig. 1. (a) Map of south Greenland and the location of Helheim Glacier (HG) and Kangerdlugssuaq Glacier (KG). The solid black curves denote the catchments of HG and KG. The locations of meteorological stations at Tasiilaq and Aputiteeq operated by the Danish Meteorological Institute (DMI) are shown in red and blue circles, respectively. Black triangles represent points where we created the SST anomaly time series. **(b)** Orthophoto from 1981 of KG draped onto the 1981 DEM. Red lines show the extent during the LIA maximum and the blue lines shows the glacier front position in 2012. **(c)** Same as **(b)** but for HG. Note that due to glacier fluctuations during the 20th century HG by 1981 was very close to its LIA maximum extent. Thinning between 1850–1981 has uncertainties of 7.2 (HG) and 13.3 m (KG).

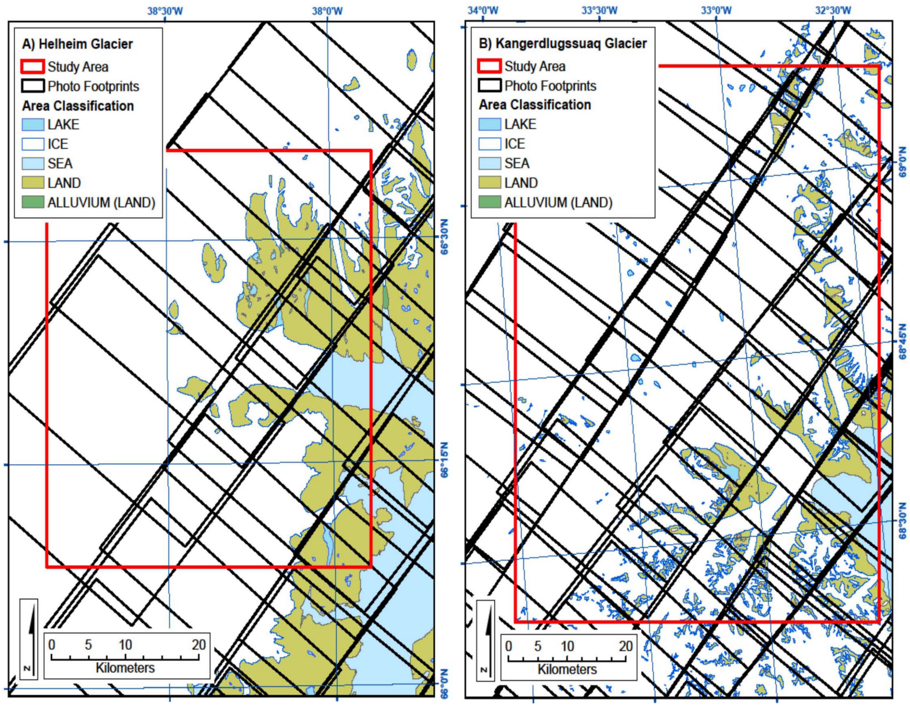

Fig. 2. Frontal portion of HG (left) and KG (right). Black lines shows photo footprints. Red polygon denotes the area for which a digital terrain model was made for this study. Digital map data is the topographical layer from GEUS' Geological map of Greenland (http://data.geus.dk/map2/geogreen/Geology.pdf).

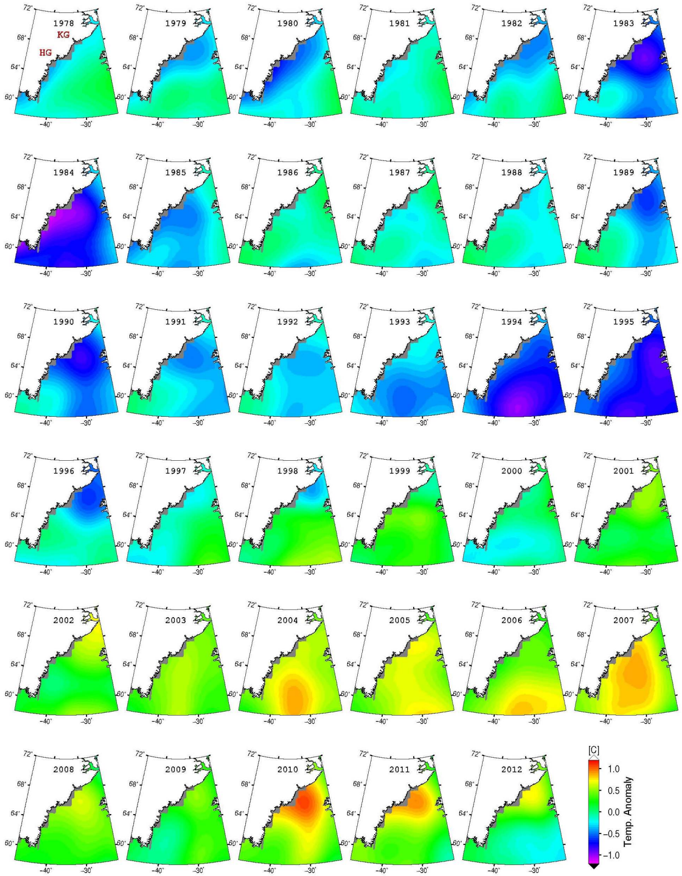

Fig. 3. Mean annual sub-surface water temperature anomalies.

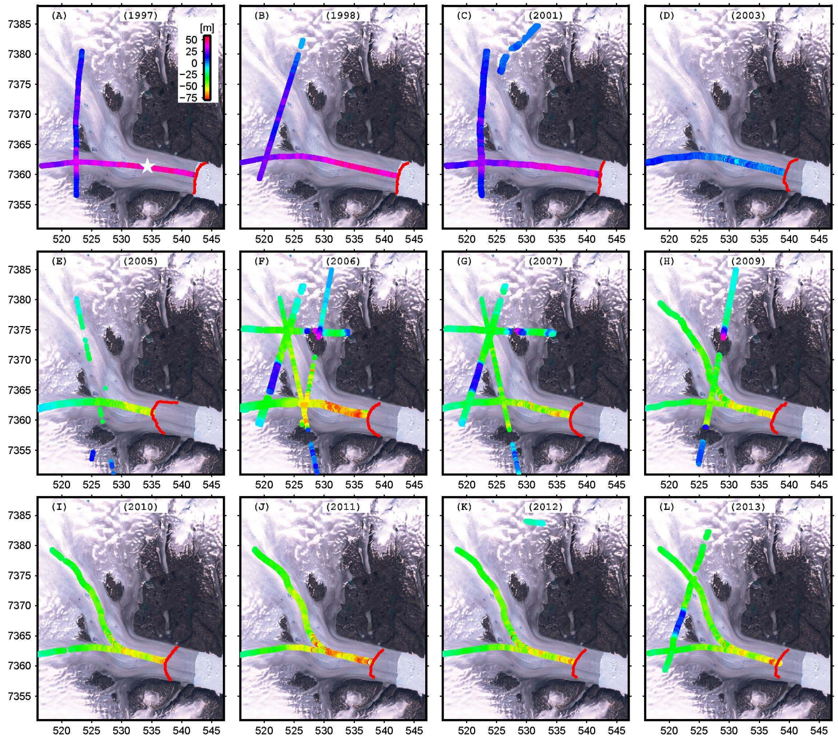

Fig. 4. Elevation changes relative to 1981 on HG. Colors indicate the change in HG elevation relative to 1981 along the track lines. The color bar is in metres. Uncertainties are 5.1 m. Areas near the glacier margin show the greatest elevation change. The red curve shows the position of the calving front. The panels show elevation changes of HG during **(a)** 1981–1997, **(b)** 1981–1998, **(c)** 1981–2001, **(d)** 1981–2003, **(e)** 1981–2005, **(f)** 1981–2006, **(g)** 1981–2007, **(h)** 1981–2009, **(i)** 1981–2010, **(i)** 1981–2011, **(k)** 1981–2012, **(l)** 1981–2013. The white star in **(a)** represents the location of the time series shown in Fig. 7a. The background map is a Landsat7 ETM+ "True color" image from 2 August 2001. The axes displays UTM zone 24 coordinates in kilometres.

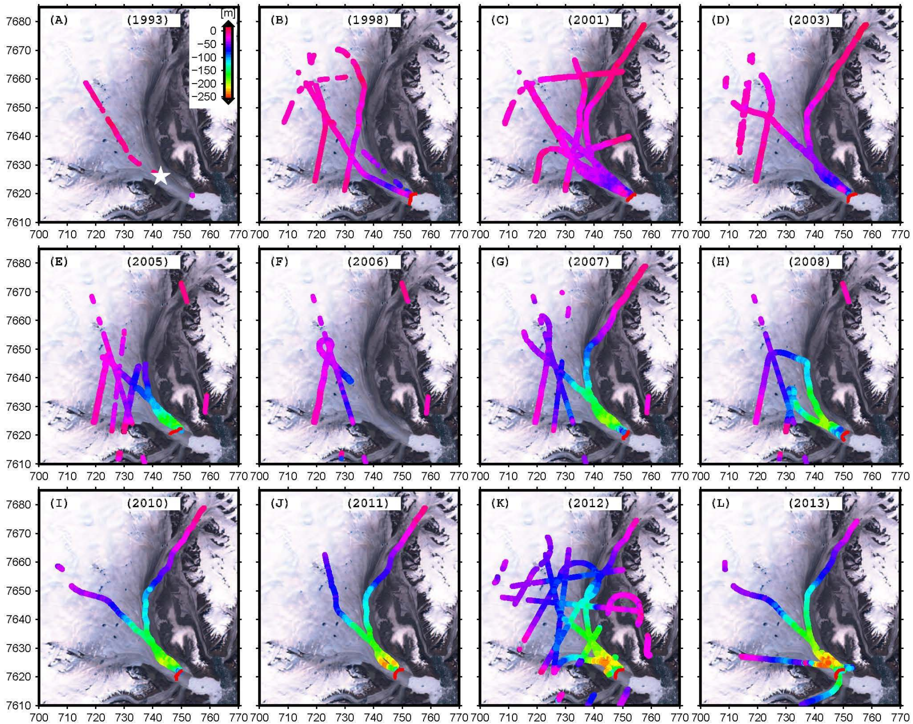

Fig. 5. Elevation changes relative to 1981 on KG. Same as for Fig. 4, but for KG. The panels show elevation changes of KG during **(a)** 1981–1993, **(b)** 1981–1998, **(c)** 1981–2001, **(d)** 1981–2003, **(e)** 1981–2005, **(f)** 1981–2006, **(g)** 1981–2007, **(h)** 1981–2008, **(i)** 1981–2010, **(j)** 1981–2011, **(k)** 1981–2012, **(l)** 1981–2013. The white star in **(a)** represents the location of the time series shown in Fig. 7b. The background map is a Landsat7 ETM+ "true color" image from 6 August 1999. The axes displays UTM zone 24 coordinates in kilometres.

TCD
8, 1257–1278, 2014

Glacier dynamics at Helheim and Kangerdlugssuaq glaciers

S. A. Khan et al.

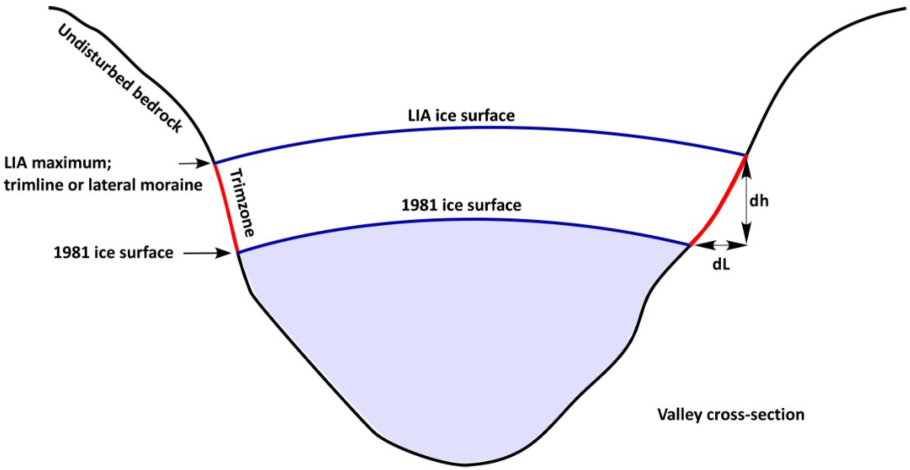

Fig. 6. Sketch of outlet glacier perpendicular to the flow direction. Points are placed at the trimline or lateral moraine marking the LIAmax position and at the 1981 ice surface. The vertical difference (dh) is the thinning each sample location.

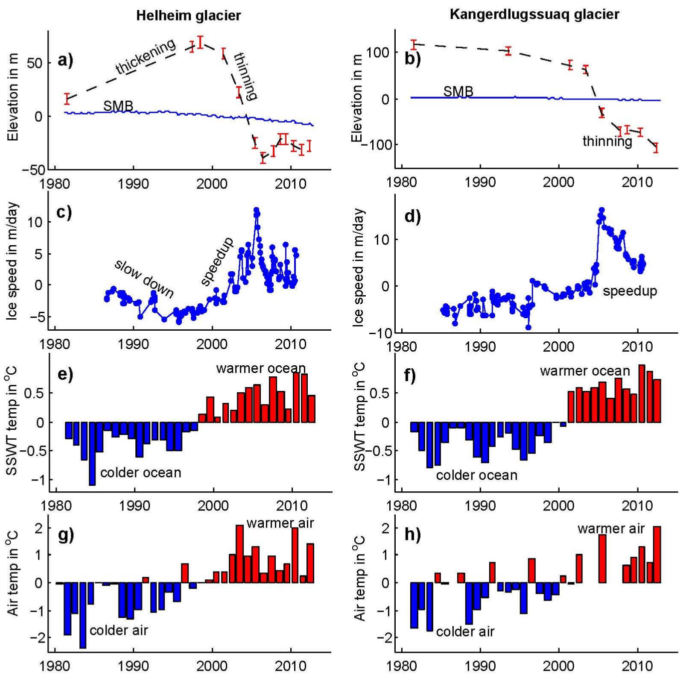

Fig. 7. Time series of surface elevation change, surface velocity, sub-surface water temperature (SSWT), and air temperature. **(a)** shows the time series of elevation change relative to 1981 of HG at the location marked by a white star in Fig. 4a. **(b)** same as for **(a)**, but for KG. Error bars of ±5.1 m (HG) and ±9.4 m (KG) are displayed in **(a)** and **(b)**, representing the combined vertical uncertainty in elevations. **(c)** and **(d)** Surface flow speed anomalies obtained from Bevan et al. (2012) for HG and KG, respectively, in m yr^{-1}, with the mean flow speed from 1995 to 2012 removed. SSWT anomaly in degrees Celsius at point 1 **(e)** and point 2 **(f)** (see Fig. 1a for locations) with the mean temperature during 1981–2012 removed. Air temperature anomaly in degrees Celsius at Tasiilaq **(g)** and at Aputiteeq **(h)** with the mean temperature during 1981–2012 removed.

TCD
8, 1257–1278, 2014

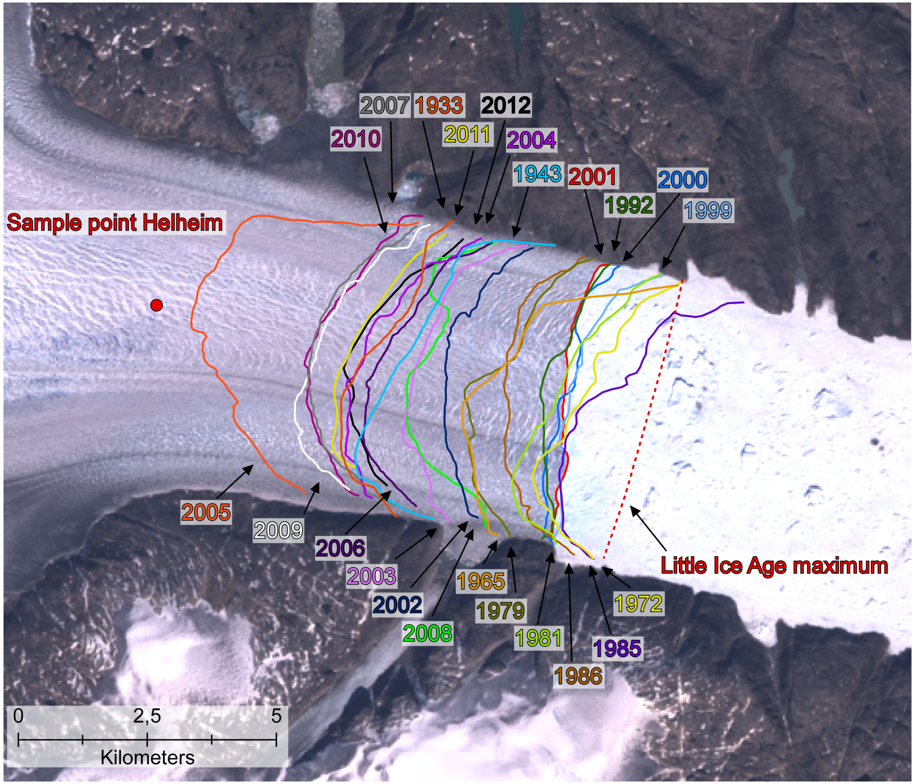

Fig. 8. Frontal position of HG. Oblique aerial image (1933), Vertical aerial image (1943), Corona satellite (1965), Landsat 1 MSS (1972 and 1979), Vertical aerial image (1981), Landsat 5 TM (1985, 1986, 1992), Landsat 7 ETM+ (1999–2012).

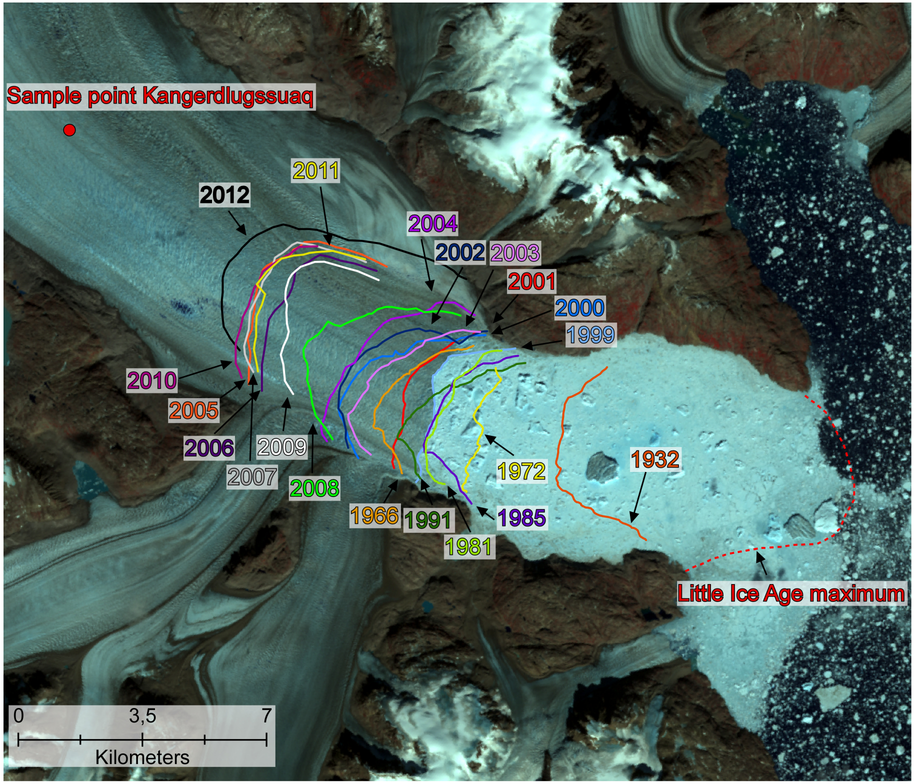

Fig. 9. Frontal position of KG obtained from Oblique aerial image (1932), Corona satellite (1966), Vertical aerial image (1972 and 1981), Landsat 5 TM (1985 and 1991), Landsat 7 ETM+ (1999–2012).

TCD
8, 1257–1278, 2014

Glacier dynamics at Helheim and Kangerdlugssuaq glaciers

S. A. Khan et al.

Title Page
Abstract
Introduction
Conclusions
References
Tables
Figures
◀I
▶I
◀
▶
Back
Close
Full Screen / Esc
Printer-friendly Version
Interactive Discussion